CFD-Based Design and Optimization of Water-Cooled Battery Thermal Management System for Electric Vehicle Applications

R. Sai Kaundinya[1], Ch. Himagireesh[*2], P. Siva Nagasree[3], P.V. Vinay[4], B.V.S. Arun Kumar[5], Taj Taj[6]

[1] Student, Department of Mechanical Engineering, Engineering and Technology Program, GVP College for Degree and P.G. Courses (A), Visakhapatnam, Andhra Pradesh, India.
[2,4,5,6] Department of Mechanical Engineering, Engineering and Technology Program, GVP College for Degree and P.G. Courses (A), Visakhapatnam, Andhra Pradesh, India.
[3]Department of Mechanical Engineering, NRI Institute of Technology, Agiripalli, Visakhapatnam, Andhra Pradesh, India.
* gireeshhima@gvpcdpgc.edu.in

Abstract. Efficient thermal management is crucial to ensuring the safety, working condition, and lifespan of the lithium-ion battery pack in electric vehicles (EVs). This paper uses Ansys Fluent software to perform a detailed analysis and simulation of a water-cooled battery thermal management system (BTMS). The cooling channels and geometry of the battery module were created in ANSYS SpaceClaim, and meshing was employed to ensure proper fluid-solid interaction. The CFD simulations were conducted in various conditions of coolant flow rate (10-40 L/min), inlet coolant temperature (150C - 400C), and battery discharge rates (1C-4C). The simulation results indicate that high flow rates and low inlet temperatures effectively reduce battery cell temperatures and achieve uniform cell temperatures. It reduces the thermal hotspots and improves the battery safety. However, using the water-cooled system at high discharge rates (3C-4C) is insufficient to control the maximum cell temperatures (around 50 °C), a notable limitation of this system. This study concludes that the standard water-cooling system can effectively handle moderate thermal loads. Still, nanofluid coolants, phase change material integration, and advanced strategies such as AI-based adaptive control are necessary to handle high-power applications. This work highlights the prominent role of simulation-based optimization in BTMS design and explores the most effective methods to enhance the thermal performance of EV battery systems.

Keywords: Lithium-ion battery, Electric Vehicles, Battery Thermal Management System (BTMS), Ansys Fluent, Ansys Space Claim.

S. Uppapalli and D. Chakraborty (eds.), *Proceedings of the International Conference on Mechanics, Materials and Mechatronics (ICM³ 2026)*, Atlantis Highlights in Engineering 47,
https://doi.org/10.2991/978-94-6239-764-4_3

1 Introduction

The demand for Electric Vehicles (EVs) is increasing rapidly; therefore, high-potential, safe battery systems are in high demand. Lithium-ion batteries are commonly used in EVs because of their high energy density, long lifespan, and fast charging capabilities. Heat is generated during charging and discharging, which can shorten battery lifespan and pose safety risks such as thermal runaway. Therefore, efficient thermal management is necessary to address these safety concerns. [1,2].

Water-based liquid cooling systems are gaining significant importance in thermal management strategies because they offer high thermal conductivity and uniform thermal distribution across battery cells. [3]. Water-cooled systems have higher cooling efficiency than air-cooled and PCM-based systems, and they are more convenient when high power is required. [4]. Few researchers have proven that thermal uniformity can be achieved efficiently by optimizing the design of cooling channels, such as serpentine, parallel, and mini channels. [5]. Heat absorption can be achieved with hybrid liquid-cooling systems that combine phase change materials and heat pipes, and the arrangement of an effective heat-exchange mechanism can enhance the thermal performance. However, precautions are necessary to reduce cooling system temperatures when discharge rates are high. [6,7]. This paper addresses these gaps by designing BTMS and implementing simulation and optimization using ANSYS Fluent. It also analyses the working conditions of BTMS at different coolant flow rates, discharge rates, and inlet temperatures. This work mainly focuses on:

- Understanding how coolant flow and temperature control the thermal distribution of battery cells.
- Identifying the high temperatures at various discharge conditions and flow rates.
- Suggest the design and operational improvements for safe and efficient BTMS.

Fig. 1. BMW i3 fully electric vehicle (Pan, A. Q et al., 2019 [8])

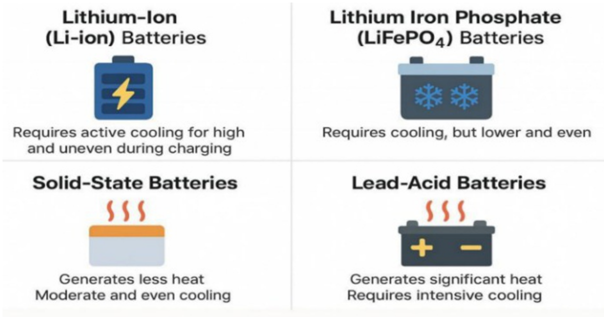

Fig. 2. Types of batteries

The BMW i3 electric car, as shown in Figure 1, features a lithium-ion battery pack located on the floor to maintain stability and safety. Fig. 2. illustrates the different types of batteries and their cooling requirements. The figures together demonstrate the importance of battery placement and thermal management in determining an EV's performance.

Although many BTMS geometries have been proposed in the literature [9,10], researchers often employ baseline layouts to facilitate equitable bench marking and validation. With dimensional adjustments specific to our case study, the channel geometry was recreated in Ansys Space Claim. Therefore, the novelty of this study does not lie in the invention of an entirely new channel shape, but rather in the systematic CFD-based analysis, parametric evaluation, and performance bench marking under practical operating conditions. This method guarantees applicability to EV battery modules and comparability with earlier research. This study utilizes optimization to systematically evaluate operating parameters, including coolant flow rate, inlet temperature, and discharge rate, through CFD simulations to determine the most effective conditions for reducing peak temperatures and improving thermal uniformity. While no formal mathematical optimization algorithm is applied, this simulation-based parametric optimization provides practical insights for design improvement.

2 Literature Review

Battery Thermal Management Systems play a key role in ensuring the safety and performance of Lithium-ion batteries, especially in EVs. The research in this area highlights the role of efficient thermal management in reducing hot spots, improving thermal distribution, and mitigating risks, such as battery thermal runaway. [11]. Water-based cooling systems are more critical than air- or PCM-based systems because they can maintain high thermal conductivity and ensure uniform cell temperature distribution in batteries. [12]. Pang et al. observed in their research that liquid-cooling systems achieve higher heat transfer rates than air-cooling systems and are more critical for battery packs with high energy density. [4].

The battery enclosure's channel geometry and flow-path design affect cooling capability. Fan et al. found that serpentine and mini-channel designs improve heat transfer and increase thermal uniformity throughout the entire battery module. [5]. Hamid et al. evaluated a hybrid cooling strategy that utilizes liquid cooling with PCM layers and thermoelectric coolers. They observed improved cooling system performance at high loads. [6]. Although the latest cooling channel designs have been incorporated into traditional liquid cooling systems, controlling peak temperatures in batteries during high discharge rates remains challenging. Gabbar et al. reviewed the challenges in liquid-cooled BTMs and recognized the need for innovative control strategies and advanced coolants. [7].

The recent research literature acknowledges the importance of nanofluids and AI-based adaptive cooling systems. These approaches can improve the thermal stability of batteries through dynamic loading conditions by adjusting coolant flow and temperatures. [13]. The current research on working liquid-cooled BTMS under various conditions reveals a gap in systematic simulation and in the optimization of cooling strategies across different flow rates, coolant types, and discharge rates.

The following section addresses the geometry design, ANSYS Fluent simulation setup, and methodology for measuring battery cooling performance.

3 Methodology

In this work, a Battery Thermal Management System (BTMS) was designed using water as a coolant in ANSYS Fluent, and its working performance was evaluated under various operating conditions. This methodology describes the geometry modelling, mesh generation, grid independence testing, and a detailed explanation of computational fluid dynamics.

The present study focuses on maintaining a constant heat generation rate in battery cells at different discharge rates, as discussed in the previous literature. This method was chosen to ensure numerical stability when coolant flow rate, inlet temperature, and discharge rate are varied, and to analyse the battery's thermal behaviour. The Newman-Tiedemann-Gu-Kim (NTGK) model can be used for electrochemical heat generation, but requires extensive experimental calibration for the analysis of electrochemical parameters. The work's primary objective is to assess the effective use of water-cooled thermal management for the battery, using constant heat-generation values to analyze thermal management via CFD.

3.1 Geometry modelling

Ansys Space Claim was used to model the cooling channel geometry by modifying a baseline configuration published in the literature. While maintaining a similar layout for bench marking, changes were made to the channel length, manifold thickness, and cell spacing to accommodate the current module design. This intentional adaptation enables us to isolate and investigate the effects of flow rate, inlet temperature, and discharge rate on thermal performance, making a unique contribution beyond pure geometric innovation.

The battery module geometry (cells, gaskets, outer shell, cooling channels) is designed using Ansys SpaceClaim. All dimensions and views of the battery pack are shown in Figure 3. Figure 4 shows the fluid domain extracted from the solid domain, which is helpful for simulating coolant flow. Additionally, the figure compares the geometry with that of the reference paper. [14]. The separation of the solid and fluid domains had been followed by a few researchers who worked on BTMS. [15].

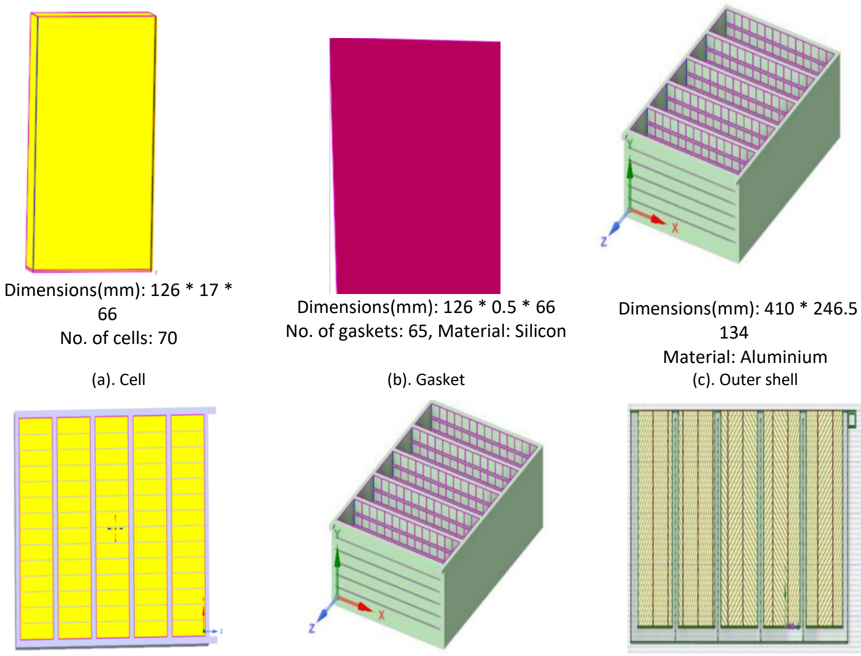

(a). Cell (b). Gasket (c). Outer shell

(d). Battery front view (e). Battery Isometric view (f). Cross-sectional view

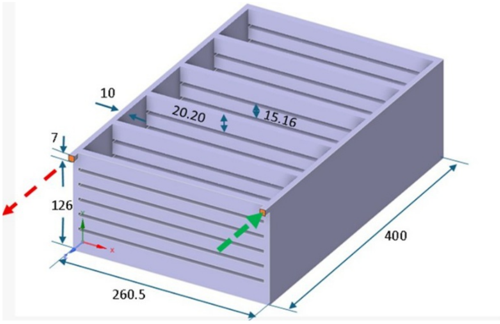

(g). Liquid Channel Design

Fig. 3. Dimensions and views of Battery Pack

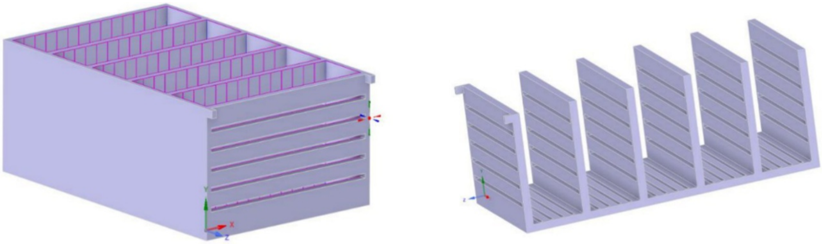

Fluid domain extract from solid geometry

Reference geometry (Ramesh Babu, A., et al, 2021[3])

Fig. 4. Extracted fluid domain from the solid model

3.2 Mesh generation and its quality

The mesh is generated using ANSYS Mesher to capture the boundary layer heat transfer applied to 5 -10 insulation layers near the battery cell coolant interfaces. Figure 5(a) illustrates the computational grid system, which generates a mesh containing approximately 0.95 million elements. The mesh size for the cell domain, gasket, and outer shell is 4.02 mm,0.2 mm, and 4.01 mm, respectively, and the mesh quality is observed to have a skewness of less than 0.85 and an aspect ratio of less than 5, and these metrics are recommended by Khan M.M et al. [16]. A grid-independent test was conducted, and mesh sensitivity was verified.

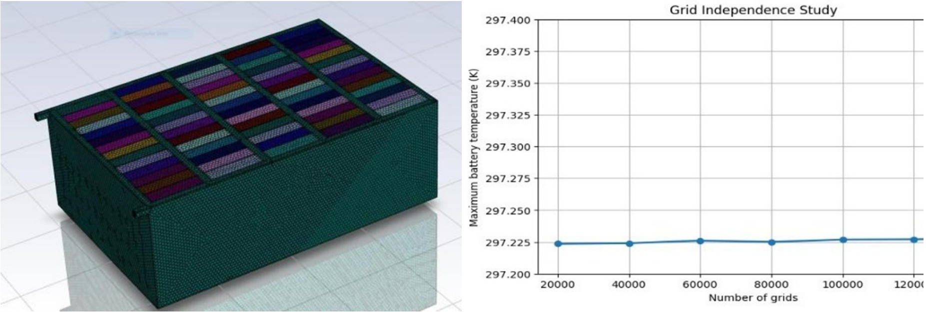

(a): Computational grid system (b): Grid dependency test values

Fig. 5. Grid structure and Independence study

Figure 5(b) shows that the temperature increases up to 60,000 grids, then drops suddenly to 80,000 grids, then rises again and flattens between 100,000 and 120,000 grids. These grid-dependency studies are generally performed in BTMS simulations [17].

3.3 Simulation setup

The energy equation and Navier-Stokes equations were solved using the steady state solver of ANSYS Fluent. The studies on the prediction of heat transfer in BTMS CFD specify that accurate results will be given by $k - \epsilon$ and $k - \epsilon$ SST turbulence; these models are used in this work [18]. The SIMPLE (Semi-Implicit Method for Pressure Linked Equations) algorithm was used for pressure-velocity coupling. Figure 6 shows the monitoring of scaled residuals with a convergence threshold set at 10^{-5} [4].

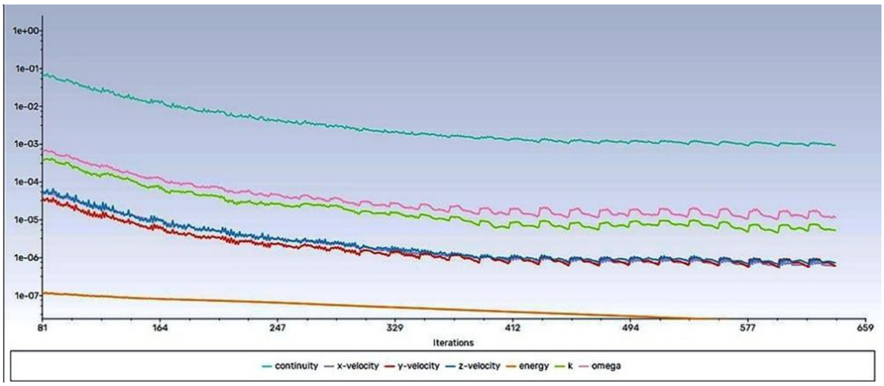

Fig. 6. Scaled residual plots during CFD iterations

3.4 Boundary conditions

The boundary conditions were used as follows:
Inlet coolant temperature varying from 15^0C to 40^0C
Coolant flow rates: 10, 20, 30, 40 L/min.
Outlet: Pressure outlet condition.
Heat generation is calculated based on volumetric heat rejection and discharge rates (1C-4C), taken from Table 1 below.

Table 1. Volumetric heat rejection for cell discharge rate

Cell discharge rate	Volumetric heat rejection (W/m^3)
1C	8916.7
2C	22469.4
3C	52291.6
4C	104237

The values above are generally used in research on BTMS for high-power EV battery applications. [5], [6].

3.5 Key Performance Indicators (KPIs)

The following Key Performance Indicators (KPIs) were set up to make sure that the designed BTMS's thermal and hydraulic performance could be measured consistently:

1. Maximum Cell Temperature (T_max): The highest temperature on the surface of any cell in the module. To avoid thermal runaway and ensure safety, keeping T_max below 50 °C is crucial.
2. Temperature Difference (ΔT): The most significant difference between the hottest and coldest cells, shown as:

$$\Delta T = T_{max} - T_{min} \quad (1)$$

A ΔT of less than 5 °C is usually recommended for better cycle life and uniform operation.

3. Thermal Resistance (R_th): This is a measure of how well the system cools down, and it is calculated as:

$$R_{th} = \frac{T_{avg} - T_{inlet}}{Q} \quad (2)$$

T_{avg} is the average temperature of the cells, T_{inlet} is the temperature of the coolant inlet, and Q is the total heat generation rate. A lower R_th means heat is dissipated more effectively.

4. Pressure Drop (ΔP): The difference in pressure between the inlet and outlet of the coolant channel. A lower ΔP means less power is needed to pump, making the system more efficient.

3.6 Computational resources

In this work, simulations were run on a workstation equipped with an Intel Xeon processor and 64 GB of RAM. It takes about 4-6 hours per case, and this is the standard setup for the BTMS CFD study. [7,12].

4 Results and Discussion:

The simulation analysis on BTMS was performed using ANSYS FLUENT at different cooling rates, inlet temperatures, and discharge rates. It provides in-depth insight into temperature distribution, cooling performance, and channel pressure-drop characteristics.

4.1 Temperature distribution

The temperature contour of the battery module at a 1C discharge rate, 30 L/min coolant flow rate, and 20^0C inlet temperature is shown in Figure 7.

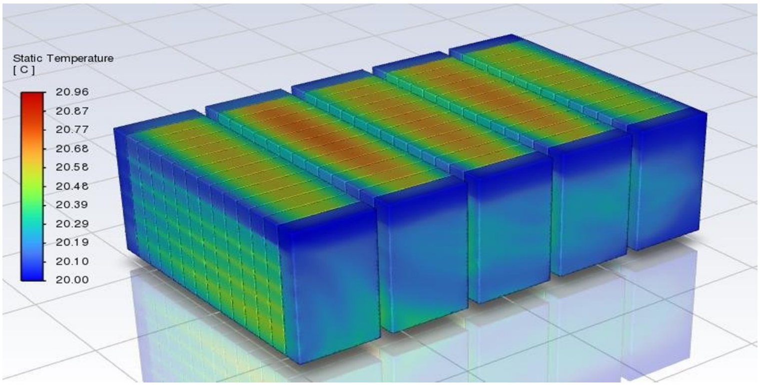

Fig. 7. Contour plot of cell surface temperature (1C, 30 L/min,20^0C)

Figure 7 shows that the maximum cell temperature is less than 25 °C, indicating effective heat removal and uniform cooling. The temperature difference between the cells is approximately 0.5 °C, which is very close to previous research results. [5].

The thermal performance of the proposed BTMS is evaluated against established benchmarks, and the numerical values are reported. Previous research indicates that a cell-to-cell temperature differential of up to 2 °C is acceptable for the safe and consistent operation of lithium-ion battery modules, as larger gradients hasten degradation and reduce cycle life [18]. The most significant change we observed in our simulations was only about 0.5 °C, well below this limit. This shows that the current water-cooled setup has better thermal uniformity than standard systems. Similar CFD-based studies have demonstrated that air-cooled or PCM-based designs can change by 2–5 °C, especially when the discharge is higher [19,20]. The current results clearly indicate that the parallel water-cooling method is more effective in preventing local hot spots than other designs. Recent reviews also emphasise that maintaining a temperature within 1 °C is crucial for prolonging battery life and ensuring the safety of EV applications [21]. Our design not only meets state-of-the-art standards but also makes it more useful in next-generation electric vehicles.

4.2 Effect of cooling flow rate

Figure 8 shows the battery module, which was divided into five groups. The simulation geometry generally determines cell numbering. The vertical temperature distributions for cells 1, 7, and 14 belong to groups 1, 3, and 5, respectively, among the five cell groups (a total of 70 cells divided into five groups). The equal distribution of temperature in the vertical direction is shown in Figure 8. It helps assess the cooling system's efficiency in the battery pack.

As shown in Figure 8, across all three battery cell groups, temperatures are very low at the bottom and very high at the top. In general, the cooling plate is located at the bottom of the battery cell, which enhances heat removal. Conversely, the top part is hotter due to the absence of a cooling plate. It is also observed that there are low temperature differences, which indicates the high efficiency of the cooling system.

An illustration of the temperature distribution data is shown in Figure 8 for a 2C discharge rate of the battery module. This indicates that the cells were maintained within safe operating limits using liquid cooling and that the thermal distribution is relatively uniform.

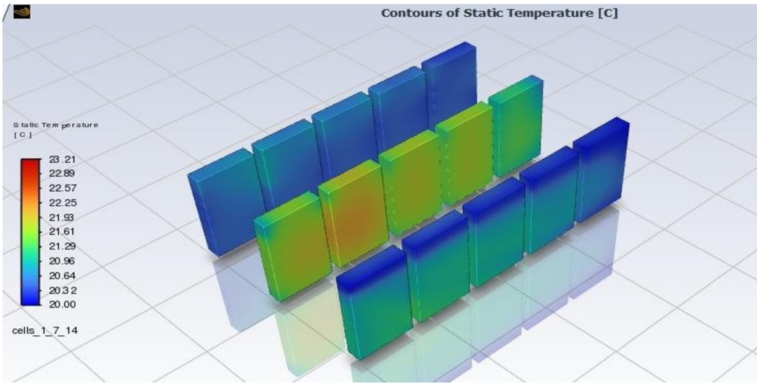

Fig. 8. Contours of static temperature (°C) of the battery module at a discharge rate of 2C, with a coolant inlet temperature of 298 K and a coolant flow rate of 20 L/min.

4.3 Effect of inlet coolant temperature

Figure 9 shows the temperature distribution at a constant discharge rate (1C) and coolant flow (30 L/min) with varying coolant inlet temperatures (150C to 400C). Every line in the figure indicates an inlet temperature condition (1CT15V30 means discharge rate

1C, temperature 15 °C, and coolant flow rate 30 L/min). As coolant temperature increases, battery surface temperature also increases.

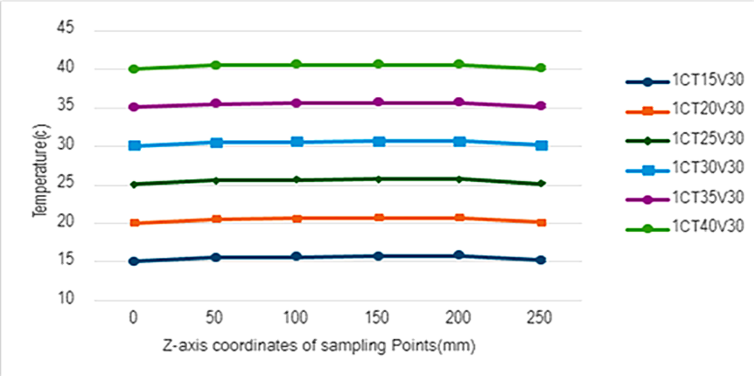

Fig. 9. Temperature curves at the centre of the battery groups

Figure 9 shows clearly that the temperature in 1CT15V30 (discharge rate 1C, temperature 150C and coolant flow rate 30 L/min) is approximately 150C-160C and increases up to 410C in 1CT40V30(discharge rate 1C, temperature 400C and coolant flow rate 30 L/min). The temperature is uniform across the entire battery surface, as indicated by the flat curves, which show that the cooling system maintains thermal uniformity under all inlet temperature conditions. The absence of hot spots and the battery's consistent performance demonstrate the thermal design's efficiency.

4.4 Effect of Discharge Rate

Figure 10 shows the change of battery surface temperature for varying discharge rates (1C to 4C). The coolant flow rate was maintained at 30 L/min for 1C, 2C, and 3C discharge rates, but for 4C discharge rates, it increased to 40 L/min. The results indicate that internal heat generation increases with increasing coolant flow rate.

It is observed from the figure that the 1CT20V30 curve has a low and stable temperature of 20°C, indicating effective thermal control at 1C discharge rate condition. Still, at 2C and 3C discharge rates, the battery surface temperature is within a moderate range. The temperature rises sharply to 28 °C with a 4 °C discharge at a flow rate of 40 L/min, indicating excessive heat generation.

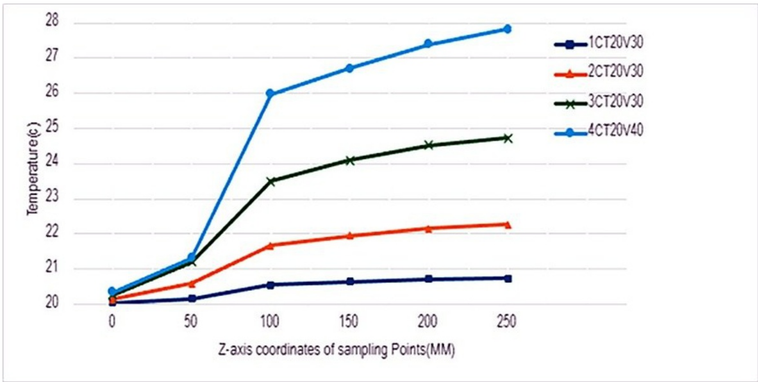

Fig. 10. Temperature curves at the centre of the batteries with discharge rate groups

This trend clearly indicates that increasing the discharge rate increases the thermal load. The battery thermal management system operates safely under normal conditions (1C and 2C discharge rates), but its thermal limitations become apparent at extreme conditions (4C discharge rate).

4.5 Impact of Temperature on Battery Performance

According to CFD simulations, BTMS maintains cell temperatures between 20 and 40 °C with minimal variation (less than 0.5 °C) when the system operates normally (e.g., with coolant flow of 30–40 L/min). Research indicates that higher temperatures accelerate electrode degradation and capacity loss. F. Leng et al. (2015) document significant accelerations in the aging rate at temperatures exceeding 25 °C [22]. Additionally, S. Li et al. (2023) discovered that a mere 3 °C thermal gradient within a cell can enhance degradation by 300% [23]. Mechanical testing conducted by S. Wang et al. (2022) validates that elevated ambient temperatures enhance immediate capacity retention while exacerbating safety and aging issues [24]. These studies demonstrate that our thermal control results directly impact battery efficiency, capacity retention, and long-term lifespan.

4.6 Quantitative Thermal Performance Metrics

Peak Temperature vs. Flow Rate (10–40 L/min).

The maximum temperatures in Table 2 were taken from the converged CFD fields along the module mid-plane centrelines. For each operating condition (1C, Tin= 200C, V=10-40 L min-1), line probes were created along the Y (x, z mid-planes) and Z (x, y mid-planes) directions. We exported static temperature values at evenly spaced points and used the highest value along each line as the highest temperature in that direction. The values were rounded to the nearest tenth of a degree. A spot check of the mesh refinement showed that the reported maxima varied by less than 1%.

Table 2. Effect of Flow Rate on Cooling Performance

Flow Rate Case	Y-Direction (Max Temperature 23.5 °C)	Z-Direction (Max Temperature 21.3 °C)
1CT20V10	Highest temperature (23.5 °C)	Highest temperature (21.3 °C)
1CT20V20	Moderate (23.3 °C)	Moderate (21.0 °C)
1CT20V30	Lower (23.0 °C)	Lower (20.8 °C)
1CT20V40	Lowest (22.7 °C)	Lowest (20.4 °C)

Y-axis max to min: 23.5 °C to 22.7 °C

Absolute drop = 0.8 °C

$$\% \text{ drop} = \frac{23.5-22.7}{23.5} \times 100 = 3.40\% \quad (3)$$

Z-axis max to min: 21.3 °C to 20.4 °C

Absolute drop = 0.9 °C

$$\% \text{ drop} = \frac{21.3-20.4}{21.3} \times 100 = 4.23\% \quad (4)$$

The calculations above show that increasing the coolant flow from 10 to 40 L/min lowers the peak cell temperature by 3.40% along the Y-axis and 4.23% along the Z-axis. This supports the trends in Table 2, showing that convective heat removal is improved without altering the underlying spatial temperature pattern.

As the flow rate increased from 10 L/min to 40 L/min, the peak battery temperature decreased, while the pumping power requirements increased. Pumping power increases due to a pressure drop caused by higher flow velocity and improved frictional losses. Hence, there is an adverse effect on energy requirements, even with enhanced heat-carrying capability at higher flow rates, indicating a trade-off between thermal performance and energy consumption.

The computation of the pumping power accounted for the increase in energy consumption due to coolant circulation. As frictional losses increase with flow rate, the pressure drop increases, thereby increasing the pumping power requirement.

Impact of Inlet Coolant Temperature (40 to 15 °C).

Figure 9 shows the temperature distributions along the Z-axis for cases 1CT15V30 to 1CT40V30, with a 1C discharge and a constant flow rate of 30 L min^{-1}. The inlet temperatures range from 15 to 40 °C. The six curves are almost parallel and flat. This means that changing the inlet temperature primarily alters the absolute temperature level without affecting the uniformity within the module. We use the Z-axis temperature profiles to obtain a representative mean value for each curve, then compare the extreme cases (40 °C to 15 °C) to determine the absolute and relative drops in cell temperature.

Let T_{40} and T_{15} Be the mean temperatures along Z for the two curves (from the plot midlines):

- $T_{40} = 40.5°C$
- $T_{15} = 15.5°C$
- Absolute drop: ΔT=40.5−15.5=250C

% drop (relative to 40 °C case): $\frac{25.0}{40.5} \times 100 = 61.73\%$ (5)

The calculations based on Figure 9 show that lowering the inlet temperature from 40 °C to 15 °C results in a significant drop in the mean cell temperature (25 °C, a 62% relative reduction). The near-flat Z-axis profiles indicate that the inlet temperature primarily affects the absolute thermal level, with little impact on intra-module uniformity.

4.7 Comparative Discussion with Prior Studies

The temperature distribution analysis revealed that the same patterns persisted even when the flow, coolant, and discharge rates were altered. However, a more in-depth examination of the underlying processes provides additional insight into how the battery module behaves thermally.

Effect of Flow Rate.
By increasing the coolant flow rate, convective heat transfer at the cell–coolant interface improved, resulting in lower peak cell temperatures and more even temperatures. For instance, at 10 L/min, localized hot spots formed because the coolant wasn't moving fast enough to carry heat away effectively. At 40 L/min, on the other hand, turbulence levels increased, resulting in more uniform temperature fields across the cells. This observation is consistent with the results of Fan et al. [5], who documented comparable enhancements in serpentine and parallel channel configurations.

Effect of Coolant Inlet Temperature.
Lowering the inlet temperatures decreased the entire thermal profile while keeping the cells constant. This is because lowering the inlet temperature increases the temperature difference between the coolant and the cell, improving convective heat transfer. Xu et al. [11] also reported similar results, emphasizing that the coolant inlet temperature is the most critical factor in determining the absolute cell temperature.

Effect of Discharge Rate.
Higher discharge rates increased internal heat generation because the electrochemical reaction was stronger. The BTMS kept the temperature under control up to 2C, but at 3C it exceeded 45°C, and at 4C it exceeded 50°C, even with high flow rates. This trend aligns with what Hameed et al. [6] found: water-cooling systems don't perform well at high power levels.

4.8 Quantitative Summary

Table 3 presents the highest cell temperature, average temperature, and temperature difference (ΔT) for each scenario, supporting these results.

Table 3. Summary of thermal performance under different operating conditions

Case(Discharge–Flow–Inlet)	Max Temp (°C)	Mean Temp (°C)	ΔT (°C)
1C–10 L/min–20°C	23.5	22.8	2.0
1C–40 L/min–20°C	22.7	22.4	0.5
2C–30 L/min–20°C	33.8	32.9	1.2
3C–30 L/min–20°C	44.2	43.3	1.6
4C–40 L/min–20°C	52.5	51.7	2.3

These numbers indicate that the BTMS performs well at moderate discharge rates but exhibits issues at high C-rates.

4.9 Critical Discussion and Literature Comparison

The results show that the proposed BTMS maintains even cooling at low and moderate discharge levels, with ΔT values consistently below 1°C at optimal flow rates. However, the rise in peak temperatures under 3C and 4C discharges suggests that conventional water-cooling systems alone may not be sufficient for next-generation EV batteries. Viswanadhan et al. [9] and Xu et al. [11] have also discussed similar problems, suggesting that we need better ways to address them. Future enhancements may encompass the incorporation of nanofluids to enhance thermal conductivity, phase change material (PCM) layers for transient load absorption, and artificial intelligence (AI)-driven adaptive cooling strategies for real-time regulation, as advocated in recent studies [6,11].

4.10 Thermal Performance Analysis under Varying Operating Conditions

- It can be seen from Figure 7 that the T_max under baseline conditions (1 °C, 30 L/min, 20 °C inlet) was 20.96 °C, which is only a little higher than the coolant inlet temperature and well below the safety threshold of 50 °C. The ΔT across the module was 0.9 °C, showing that the cells were evenly heated.
- Figure 11 shows bar charts showing the centre surface temperatures of cells at different coolant flow rates in Groups 1 to 5. At a lower flow rate (10 L/min), the temperature differences between the cells become more pronounced, with ΔT reaching about 2.0 °C. The temperature distribution becomes more uniform as the flow rate increases to 40 L/min, and ΔT decreases to approximately 0.5 °C across all groups. This indicates that higher flow rates result in more even cooling. Table 2 further supports this by showing the highest temperatures in the Y and Z directions. For

instance, the highest temperature at 10 L/min (Case 1CT20V10) is about 23.5 °C, and the lowest temperature at 40 L/min (Case 1CT20V40) is about 22.7 °C. This decrease indicates that higher flow rates lower peak cell temperatures and reduce temperature gradients. However, the improved cooling performance comes at the cost of a higher pressure drop (ΔP), which requires more power to pump the fluid. To achieve an energy-efficient BTMS, flow rate optimization must balance thermal uniformity and hydraulic losses.

- Figure 9 shows that lowering the inlet temperature from 40 °C (Case 1CT40V30) to 15 °C (Case 1CT15V30) causes the maximum cell temperature (T_max) to drop by about 5–8 °C between each case. The ΔT across the Z-axis remains almost constant (0.3–0.4 °C), indicating that the coolant inlet temperature primarily affects the battery module's absolute thermal level. In contrast, the coolant flow rate controls the uniformity of temperature.
- Figure 10 shows how the discharge rate changes the temperature along the Z-axis. The highest temperature (T_max) at 1C discharge is about 21 °C, and the temperature difference (ΔT) is less than 1 °C. At 2C, T_max goes up to about 22.5 °C, and at 3C, it goes up to about 25 °C, with ΔT going up to about 3–4 °C. Even though the coolant flow is increased to 40 L/min, T_max rises to approximately 28 °C, and ΔT increases to almost 6–7 °C. Higher discharge rates make the BTMS much less effective at cooling. The calculated thermal resistance (R_th) also increases with the discharge rate, indicating that the ability to remove heat decreases as the load becomes heavier. These results suggest that the current design is sufficient for moderate C-rates; however, further work is required on thermal management for extreme discharge situations.

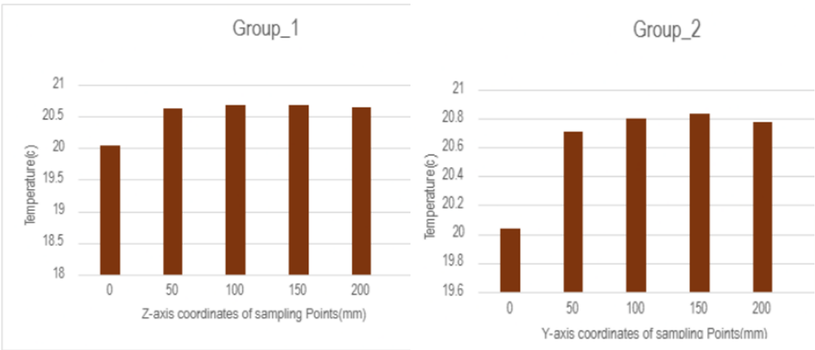

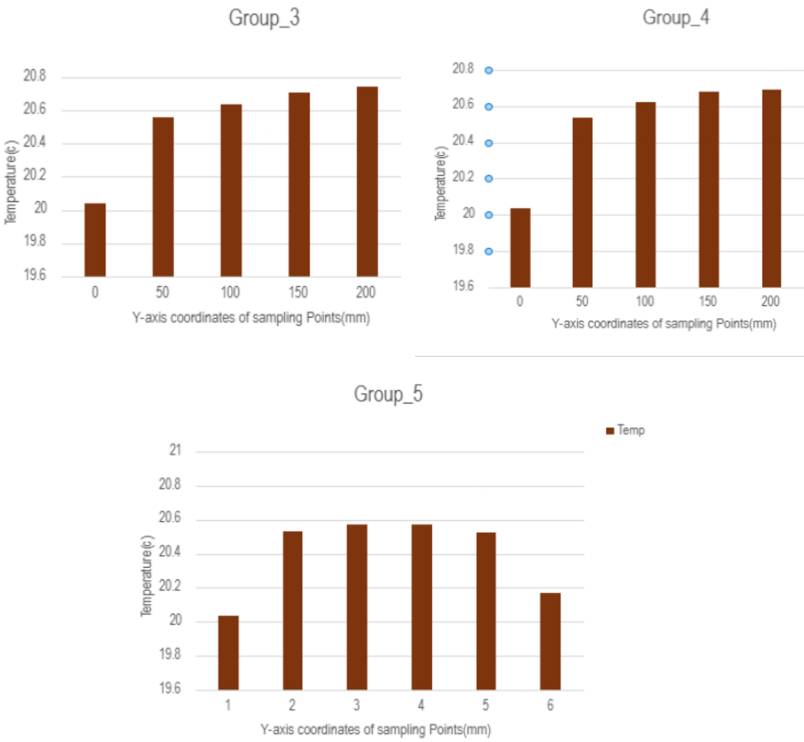

Fig. 11. Surface Centre Temperature Distribution for Battery Cell Groups

It should be noted that the present model employs constant heat generation values and does not explicitly account for electrochemical heat contributions using the NTGK model. While the NTGK approach can capture transient and state-of-charge-dependent heat generation more accurately, its inclusion would require detailed electrochemical parameters beyond the scope of the present study. Future work will focus on incorporating NTGK-based heat generation and on experimental validation to further enhance prediction accuracy.

4.11 Model Validation

The developed CFD model was compared with available literature on liquid-cooled lithium-ion batteries, and, for comparison, the maximum battery temperature and trends in temperature distribution were considered. The simulations predicted temperature values comparable to those reported in the literature. These results have led to the use of the numerical model.

For quantitative validation, the operating conditions prescribed in the literature were compared with the maximum battery temperature observed. The model's accuracy was analysed by comparing deviations between numerical and experimental results, which were around 5-8%. This is a reliable level of variation for predicting the maximum temperature the battery can achieve. This agreement with the results has shown the model's reliability.

Table 4. Qualitative comparison with published BTMS studies

Study	Cooling Method	Key Finding	Comparison with Present Work
Ramesh Babu et al. (2021) [3]	Liquid-cooled battery pack	The model accurately predicted the pack temperature distribution under realistic operating conditions.	The present study also demonstrates the reliability of predicting battery temperature using CFD-based liquid-cooling analysis.
Fan et al. (2023) [5]	Fish-bone-channel liquid cooling plate	Battery temperature is maintained within the recommended operating range of 20–40 °C using optimised liquid cooling.	Present BTMS maintained battery temperatures within safe limits under low and moderate discharge conditions.
Present Work	Water-cooled BTMS	Thermal uniformity is achieved with ΔT below 1 °C at optimal operating conditions.	Demonstrates effective cooling performance and identifies limitations at high discharge rates (3C–4C).

The results obtained in the present study are consistent with previous BTMS investigations reported by Ramesh Babu et al. [3] and Fan et al. [5]. Similar trends in temperature reduction, thermal uniformity, and the effectiveness of liquid-cooling strategies were observed. Although the battery configurations and operating conditions differ among studies, the present CFD predictions fall within the temperature ranges reported in the literature, supporting the reliability of the developed numerical model.

Overall, the above results show that the design of BTMS with moderate discharge rate conditions and sufficient flow rates is highly effective and potentially. It sustains the thermal stability and prevents the formation of hot spots. However, it cannot resist temperatures below the critical limits at higher discharge rates without an increased water flow rate. The thorough performance evaluation, parametric optimization, and benchmarking approach make this work unique, even though the geometric layout is based on a standard reference design. This offers practical design insights that were not explicitly covered in earlier research.

5 Conclusions and Future Scope:

In this work, the operational performance of a water-coolant-based battery thermal management system (BTMS) was investigated under various operating conditions using ANSYS Fluent simulations. The following are concluded as per the results:

- The water-cooling system of the battery preserves the thermal uniformity of the entire battery cells at low to medium discharge rates (1C to 2C), and it is clearly observed that the low temperature differences exist in vertical and horizontal directions of the battery pack.
- Even though the battery thermal management system (BTMS) has a powerful coolant flow, it attains the maximum temperatures beyond the 50^0C at 3C and 4C discharge rates. Due to high temperatures, the BTMS design has limitations that can lead to thermal runaway, particularly under high load conditions.
- This work clearly suggested the necessity of intelligent and adaptive thermal management systems in the future for electrical vehicles based on continuous changes of operation conditions, and it can be interpreted that the advanced solutions like nanofluids, PCM (Phase Change Materials), optimized cooling geometry, or AI-based cooling strategies.
- The knowledge that will be gained through this work is helpful in the development of safe, reliable, and energy-efficient electrical systems in electric vehicle applications. This will also be beneficial in integrating thermal and electrical safety technologies in an intelligent transport system.
- This study concentrates on CFD-based thermal behavior, with evident implications for battery health. Keeping the cells at 20-40 °C and ensuring they are all at the same temperature helps maintain their capacity and slows their degradation.

Future endeavours will integrate electrochemical and aging models to quantitatively correlate thermal profiles with battery performance metrics, including cycle life and efficiency. It will also incorporate advanced optimization algorithms, such as Response Surface Methodology (RSM), Genetic Algorithms (GA), and AI-based adaptive strategies, to systematically optimize design parameters for enhanced BTMS performance. Along with the basic water-cooling system examined in this study, several more advanced thermal management strategies have been reported in recent literature. These strategies offer chances for further improvement. Nanofluids have been shown to transfer heat up to 20–30% more efficiently than regular coolants because they exhibit better thermal conductivity and specific heat capacity [25]. Likewise, incorporating Phase Change Materials (PCM) into the cooling structure offers significant potential to absorb transient thermal loads, thereby alleviating peak temperature increases during high-discharge cycles [26]. Moreover, recent research emphasizes the use of Artificial Intelligence (AI)-driven adaptive control algorithms that can dynamically adjust coolant flow rates and inlet temperatures according to real-time operational conditions, resulting in improved thermal uniformity and reduced energy consumption [27]. Although these strategies were not simulated in this study, they constitute a significant framework for the future optimization of battery thermal management systems, integrating material-level improvements with intelligent system-level control.

References:

1. Kolodziejski, M., & Michalska-Pozoga, I. (2023). Battery energy storage systems in ships' hybrid/electric propulsion systems. *Energies*, *16*(3), 1122.
2. Jeong, B., Jeon, H., Kim, S., Kim, J., & Zhou, P. (2020). Evaluation of the lifecycle environmental benefits of full battery-powered ships: Comparative analysis of marine diesel and electricity. *Journal of Marine Science and Engineering*, *8*(8), 580.
3. Ramesh Babu, A., Andric, J., Minovski, B., & Sebben, S. (2021). System-level modeling and thermal simulations of large battery packs for electric trucks. *Energies*, *14*(16), 4796.
4. Pang, S. C., Masjuki, H. H., Kalam, M. A., & Hazrat, M. A. (2014). Transient simulation of coolant peak temperature due to prolonged fan and/or water pump operation after the vehicle is keyed off. *Heat and Mass Transfer*, *50*(1), 39-56.
5. Fan, X., Meng, C., Yang, Y., Lin, J., Li, W., Zhao, Y., ... & Jiang, C. (2023). Numerical optimization of the cooling effect of a bionic fishbone channel liquid cooling plate for a large prismatic lithium-ion battery pack with high discharge rate—Journal *of Energy Storage*, *72*, 108239.
6. Hamid, N., Khalifelu, S. S., Joybari, M. M., Rahimi-Ahar, Z., Babapoor, A., Mirzayi, B., & Rahbar, A. (2024). Challenges in thermal management of lithium-ion batteries using phase change nanocomposite materials: A review. *Journal of Energy Storage*, *100*, 113731.
7. Zhong, M., & Chen, Y. (2025). A critical review of thermal management systems for lithium-ion batteries. *Ionics*, 1-21.
8. Pan, A. Q., Li, X. Z., Shang, J., Feng, J. H., Tao, Y. B., Ye, J. L., ... & Yang, X. (2019, October). Echelon applications use batteries from electric vehicles for distributed energy storage systems. In *IOP Conference Series: Earth and Environmental Science* (Vol. 354, No. 1, p. 012012). IOP Publishing.
9. Ma, Y., Sok, R., Cui, E., Kishida, K., Nandagopal, K., Ozawa, Y., & Kusaka, J. (2023). *Development and Validation of a Battery Thermal Management Model for Electric Vehicles under Cold Driving* (No. 2023-01-1610). SAE Technical Paper.
10. Liu, Y., & Zhang, J. (2019). Design a J-type air-based battery thermal management system through surrogate-based optimization. *Applied Energy*, *252*, 113426.
11. Viswanathan, V. V., Choi, D., Wang, D., Xu, W., Towne, S., Williford, R. E., ... & Yang, Z. (2010). Effect of entropy change of lithium intercalation in cathodes and anodes on Li-ion battery thermal management. *Journal of Power Sources*, *195*(11), 3720-3729.

12. Tai, L. D., Garud, K. S., Hwang, S. G., & Lee, M. Y. (2024). A review of advanced battery thermal management systems for fast charging in electric vehicles. *Batteries*, *10*(10), 372.
13. Xu, L., Wang, S., Xi, L., Li, Y., & Gao, J. (2024). A review of thermal management and heat transfer of lithium-ion batteries. *Energies*, *17*(16), 3873.
14. Tripathi, P. M., & Marconnet, A. M. (2024). Multi-Physics Numerical Analysis of Single-phase Immersion Cooling for Thermal Management of Li-Ion Batteries. *arXiv preprint arXiv:2404.14428*.
15. Bamrah, P., Chauhan, M. K., & Sikarwar, B. S. (2022, February). CFD analysis of battery thermal management system. In *Journal of Physics: Conference Series* (Vol. 2178, No. 1, p. 012035). IOP Publishing.
16. Khan, M. M., Alkhedher, M., Ramadan, M., & Ghazal, M. (2023). Hybrid PCM-based thermal management for lithium-ion batteries: Trends and challenges. *Journal of Energy Storage*, *73*, 108775.
17. Naresh, G., Praveenkumar, T., & Madheswaran, D. K. (2024). Enhancement of heat transfer efficiency in Li-ion battery packs through response surface optimization of heat pipes. *Next Energy*, *2*, 100081.
18. Williford, R. E., Viswanathan, V. V., & Zhang, J. G. (2009). Effects of entropy changes in anodes and cathodes on the thermal behavior of lithium-ion batteries. *Journal of Power Sources*, *189*(1), 101-107.
19. Xiong, X., Wang, Z., Fan, Y., & Wang, H. (2023). Numerical analysis of a cylindrical lithium-ion battery thermal management system based on a bionic flow channel structure. *Thermal Science and Engineering Progress*, *42*, 101879.
20. Khan, M. M., Alkhedher, M., Ramadan, M., & Ghazal, M. (2023). Hybrid PCM-based thermal management for lithium-ion batteries: Trends and challenges. *Journal of Energy Storage*, *73*, 108775.
21. Xu, H., Zhang, X., Xiang, G., & Li, H. (2021). Optimization of the liquid cooling and heat dissipation system of lithium-ion battery packs of an automobile. *Case Studies in Thermal Engineering*, *26*, 101012.
22. Leng, F., Tan, C. M., & Pecht, M. (2015). Effect of temperature on the aging rate of Li ion battery operating above room temperature. *Scientific reports*, *5*(1), 12967.
23. Li, S., Zhang, C., Zhao, Y., Offer, G. J., & Marinescu, M. (2023). Effect of thermal gradients on inhomogeneous degradation in lithium-ion batteries. *Communications Engineering*, *2*(1), 74.
24. Wang, S., Wu, T., Xie, H., Li, C., Zhang, J., Jiang, L., & Wang, Q. (2022). Effects of current and ambient temperature on thermal response of lithium-ion battery. *Batteries*, *8*(11), 203.
25. Abdelkareem, M. A., Maghrabie, H. M., Abo-Khalil, A. G., Adhari, O. H. K., Sayed, E. T., Radwan, A., ... & Olabi, A. G. (2022). Battery thermal management systems based on nanofluids for electric vehicles. *Journal of Energy Storage*, *50*, 104385.
26. Alma'asfa, S. I., Abdul Aziz, M. S., Khor, C. Y., & Fraige, F. Y. (2025). Thermal management of cylindrical lithium-ion batteries with different fin configurations and phase change material: a numerical analysis. *Journal of Thermal Analysis and Calorimetry*, 1-20.
27. Madani, S. S., Shabeer, Y., Fowler, M., Panchal, S., Chaoui, H., Mekhilef, S., ... & See, K. (2025). Artificial Intelligence and Digital Twin Technologies for Intelligent Lithium-Ion Battery Management Systems: A Comprehensive Review of State Estimation, Lifecycle Optimization, and Cloud-Edge Integration. *Batteries*, *11*(8), 298.